Express Polymer Letters Vol.17, No.5 (2023) 527–545
Available online at www.expresspolymlett.com
https://doi.org/10.3144/expresspolymlett.2023.39

Research article

A new testing strategy based on the wetting concept for characterizing rubber-filler interaction in rubber compounds and its application to the study of the influence of epoxy groups and non-rubber components on rubber-filler interaction in natural rubber compounds

Hai Hong Le[1*], *Tung Xuan Hoang*[1], *Syed Bilal Haider*[2], *Subhradeep Mandal*[1], *Uta Reuter*[1], *Kedar Dhakal*[3], *Rameshwar Adhikari*[3], *Katrin Reincke*[4], *Subhan Saleah*[5], *Sven Wiessner*[1,6]

[1]Leibniz-Institut für Polymerforschung Dresden e.V., D-01069 Dresden, Germany
[2]Martin-Luther University Halle-Wittenberg, 06108 Halle, Germany
[3]Central Department of Chemistry, Tribhuvan, University, Kirtipur, Kathmandu, Nepal
[4]Applied Science University Merseburg, 06217 Merseburg, Germany
[5]Department of Rubber Technology and Polymer Science, Prince of Songkla University, 94000 Pattani, Thailand
[6]Institute of Materials Science, Technische Universität Dresden, D-01062 Dresden, Germany

Received 12 September 2022; accepted in revised form 13 December 2022

Abstract. In the present work, a new testing strategy was proposed to characterize the effect of a functional group on the interaction between rubber and filler in a rubber compound. In principle, the filler is mixed into a blend of rubber A and rubber B produced by functionalizing the rubber A with a specific chemical group. The phase-selective wetting of the filler is directly related to the effect of the functional group. Based on the new test approach, the impact of the non-rubber components in natural rubber (NR) and its epoxidation on the rubber-filler interaction in carbon black (CB) filled NR compounds was investigated. Accordingly, CB was mixed in three blends consisting of NR/isoprene (IR), deproteinized natural rubber (DPNR)/IR, and NR/epoxidized natural rubber (ENR). The phase selective wetting of CB was quantitatively characterized based on the *wetting concept*. It was found that proteins and epoxy groups did not affect the affinity between NR and CB, while the linked phospholipids interacted with the CB surface through cation-π bonding. By fitting the experimentally determined selective wetting of CB into the *Z-model*, the corrected surface tension of NR describing the effect of phospholipids was determined. The proposed test strategy was applied to other NR blends filled with silica and the hybrid CB/silica filler as reference fillers to demonstrate its transferability and verification.

Keywords: *rubber, rubber blends, rubber-filler interaction, selective filler wetting, flocculation*

1. Introduction

Carbon black (CB) is widely used as a filler to reinforce rubber compounds and blends. In particular, CB-filled natural rubber (NR) is an indispensable component in the truck tire industry due to its good abrasion resistance and reinforcement [1]. Despite the tremendous advantages of silica/silane systems, NR/CB compounds are still used today for the tread and inner parts, such as belts and sidewalls, regardless of the vehicle type. The mechanical properties of CB-reinforced rubber composites are largely controlled by the extent of interfacial adhesion between CB and rubber [2]. In general, the interaction of rubber with CB is predominantly determined by the

*Corresponding author, e-mail: le-haihong@ipfdd.de

physical adsorption, *i.e.* the entanglement of rubber molecules on the carbon black [3]. The structural defects, impurities, and chemical groups on the CB surface have the potential to become active sites that can interact well with rubber and improve rubber performance [4, 5]. Efforts have been made to improve the rubber-filler interaction to achieve the optimum performance of CB-filled rubber compounds. The main methods to improve the interaction between CB and rubber include the addition of a coupling agent [6, 7], chemical modification of rubber [8] and surface modification of filler [4, 9–11]. The improvement of rubber-filler interaction can be demonstrated by studying the mechanical properties such as tensile tests or dynamic mechanical analysis (DMA) [4, 7]. It can be characterized by optical microscopy, transmission electron microscopy (TEM), and TEM network visualization process [12], as well as scanning transmission electron microscopy combined with electron energy loss spectroscopy (STEM-EELS) [13]. The formation of rubber-filler interphase can be characterized by the bound rubber measurement [14] and spectroscopic techniques such as X-ray photoelectron spectroscopy [15], X-ray-induced Auger electron spectroscopy [16], Nuclear magnetic resonance (NMR) [14], and Raman spectroscopy [17].

The reinforcement potential of furnace carbon black is closely related to the amount of highly energetic sites, which decreases significantly with treatment temperature and disappears almost completely during graphitization [11]. In addition, the functional groups on the surface of graphitized CB have entirely disappeared due to the very high processing temperature [18]. As a result, graphitized CB shows very low affinity to synthetic rubbers such as ethylene propylene diene monomer rubber (EPDM) [19], styrene-butadiene rubber (SBR) and polybutadiene rubber (BR) [20] as well as isobutylene-isoprene rubber (IIR) [21]. This behavior seems to be in contrast to that of the NR. Take a close-up look at the NR compound filled with furnace CB, a poor NR-CB interaction can be evidenced by taking into consideration the phase selective filler localization of CB in NR blends. For example, in NR/acrylic rubber (ACM) blend [22] and NR/butadiene rubber (BR) blends [23, 24] only an insignificant amount of furnace CB such as N330 and N220 was found in the NR phase. However, after the graphitization process, the interaction of NR with graphitized CB becomes stronger, as found by Schwartz *et al*. [25]. They studied the CB flocculation process of NR compound filled with standard CB N229 and graphitized one and found that the flocculation process becomes much weaker after CB graphitization, which may indicate a better interaction between NR and graphitized CB. The physical background for the difference in rubber-filler interaction of NR compared to synthetic rubbers before and after graphitization has not been investigated. In our previous work [26], bromobutyl rubber (BIIR)/natural rubber (NR) blends filled with conductive carbon black/silica hybrid filler were prepared as self-healable flexible composites. The phase-specific wetting and location of the hybrid filler of CB/silica in rubber blends were determined experimentally using a newly developed *wetting concept*. Accordingly, the filler surface fraction wetted by different rubbers of the blend can be quantified by Fourier transform infrared spectroscopy (FTIR) investigation of the bound rubber. The results showed that the conductive CB used was mainly wetted by the NR phase, which is consistent with the results of graphitized CB reported in [25]. Compared to furnace blacks, the conductive carbon black used in [26] is produced at much higher temperatures. As a result, a much larger fraction of well-ordered structure and very few defects were observed for conductive CB, which is similar to graphitized CB [18, 27]. One possible explanation for the good interaction between the graphite-like surface of conductive CB and NR could be the presence of the non-rubber components in NR, such as proteins and phospholipids. Compared to synthetic rubbers, NR is made up of isoprene units with phospholipids and proteins linked to two terminals of the molecule [28, 29]. Some papers [30–32] have already reported the effects of non-rubber components on the vulcanization kinetics, storage hardening and gel formation of NR during accelerated storage under various conditions. However, the question of why the conductive CB and graphitized CB have a high affinity to NR but not to other synthesis rubbers has not been answered so far.

In the present work, a new strategy was proposed to identify the non-rubber components mainly responsible for the strong rubber-filler interaction in conductive CB-filled NR compounds. According to this strategy, the filler is blended into a mixture of rubber A and rubber B, which is prepared by functionalizing rubber A with a specific chemical group. The phase selective wetting of the filler is determined experimentally and is directly related to the effect of the

functional group. Specifically, CB was blended in three compounds consisting of NR/isoprene (IR), deproteinized natural rubber (DPNR)/IR and NR/ epoxidized NR (ENR). IR is a 'pure' rubber with isoprene units in the backbone without functional groups. NR consists of an isoprene backbone and phospholipids and proteins attached to two ends of the molecule. DPNR contains only phospholipids at one end because the proteins have been almost completely removed by a deproteinization process. ENR contains phospholipids at one end and epoxide groups along the molecule. The proteins were removed during epoxidation. The reason for including ENR is to test the applicability of the new test strategy for different compounds. In addition, ENR has been widely used to improve the rubber-filler interaction in filled NR compounds. The results of the present work can verify the suitability of ENR as a coupling agent for filled NR compounds. The phase selective wetting of CB was quantitatively characterized using the *wetting concept*. Based on the selective wetting of CB, the rubber-CB affinity can be discussed and the role of non-rubber components and epoxy groups can be distinguished. Unlike CB with a hydrophobic surface, silica has hydrophilic surface properties and was used as a reference filler. The result of the rubber-filler interaction characterized by the new test strategy was discussed, considering the results reported in the literature obtained by different testing methods. The extent of rubber-filler interaction determined by the proposed test strategy was used to predict the filler wetting in other natural rubber blends to demonstrate the transferability and verification of the method.

2. Materials and experimental

2.1. Materials and mixture preparation

Natural rubber (NR) (Standard Vietnamese Rubber (SVR 10), Weber & Schaer GmbH) with a protein content of 6.0 wt% and synthetic polyisoprene (IR) (Cariflex JR 309, Shell Chemical Co.) with 95.0 wt% cis-1,4 isoprene units were used. Epoxidized natural rubber (ENR) with 50% epoxidation (Epoxiprene, Muang Mai Guthrie PCL, Thailand) and brominated isobutene-isoprene rubber (BIIR) (LANXESS X_Butyl™ BB X2, Lanxess AG, Germany) with a halogen content of 1.95 wt% were used.

Deproteinization of high ammonia (HA) concentrated latex was performed according to the procedure described by Chaikumpollert *et al*. [33]. HA concentrated latex with 60.0 wt% dried rubber content (DRC) was purchased from Yala Latex Co., Ltd. (Thailand). Urea, acetone, and sodium dodecyl sulfate (SDS) were purchased from Sigma-Aldrich. Firstly, HA latex was mixed with urea (0.1 wt%), acetone (2.5 wt%), and sodiumdodecylsulfate (SDS) (1.0 wt%). The mixture was then incubated for 12 hrs and followed by centrifugation at 8000 rpm for 45 min. The cream fraction was collected and re-dispersed in water to obtain 30% DRC latex in the presence of SDS (1.0 wt%). The diluted latex was again centrifuged twice with a similar condition to the first step. The final diluted latex was coagulated with methanol and dried in the oven at 50 °C until constant weight. NR and DPNR were masticated by means of a two-roll mill in order to reduce their Mooney viscosity to the range of IR.

Conductive carbon black (Printex XE-2B, Orion Engineered Carbons GmbH, Germany) and silica (Ultrasil 7000 GR, Evonik Industries AG, Germany) were used as filler. The properties of rubbers and fillers used are listed in Table 1 and 2.

An internal mixer (Thermo HAAKE Rheocord Polylab 300p System, Thermo Fisher Scientific Inc.) was used to prepare the filled blends, keeping the following mixing conditions: an initial chamber temperature (T_A) of 50 °C, a rotor speed of 60 rpm, and a fill factor of 0.68. A conductivity sensor system was

Table 2. Properties of CB and silica.

Filler	Surface area (BET) [m^2/g]	Particle size [nm]	Carbon [wt%]	Surface tension [mN/m]
CB	1000 [18]	27	100 [18]	28 [26]
Silica	160	10	0	72 [37]

Table 1. Properties of rubbers used.

Rubber	Protein [wt%]	Phospholipid [wt%]	Epoxidation [mol%]	Mooney viscosity ML(1+8), 125 °C, MU	Surface tension [mN/m]
NR	6.00	1	0	N/A	22.0 [34]
DPNR	0.68	1	0	N/A	20.0 [34]
ENR	0.80	1	50	90	30.6 [35]
IR	0	0	0	42	20.0 [34]
BIIR	0	0	0	46	25.5 [36]

Table 3. Formulation of rubber compounds filled.

Single compound	Quantity [phr]					
	NR	DPNR	ENR	IR	CB	Silica
S1	100				10	
S2		100			10	
S3			100		10	
S4				100	10	
S5	100					50
S6		100				50
S7			100			50
S8				100		50

Table 4. Formulation of rubber blends filled with CB and silica, respectively.

Blend	Quantity [phr]					
	NR	DPNR	ENR	IR	CB	Silica
B1	50			50	10	
B2		50		50	10	
B3	50		50		10	
B4	50			50		50
B5		50		50		50
B6	50		50			50

Table 5. Formulation of rubber blends filled with hybrid filler CB/silica.

Blend	Quantity [phr]						
	BIIR	NR	DPNR	ENR	IR	CB	Silica
B7	70	30				3	3
B8	70		30			3	3
B9	70			30		3	3
B10	70				30	3	3

installed in the chamber of the internal mixer to measure the electrical signal of the conductive mixtures. The total mixing time was kept constant at 30 min. During the mixing time, a small piece of the compound was taken at 5, 7, 10, 15, 20, 30 min for further investigation.

The formulation for the preparation of rubber compounds and blends is given in Tables 3, 4 and 5.

2.2. Experimental determination of filler wetting in rubber compounds and blends

For the investigation of the rubber-filler gel of the compounds and blends, for example, from NR and IR, 0.2 g of each raw mixture was stored for seven days in 100 ml xylene at room temperature. The rubber-filler gel was collected and dried up to a constant mass. The rubber content in the gel L^{NR} and L^{IR} as well as $L^{NR/IR}$ as a measure for the wetting behavior of the filler surface, for example, CB, by NR and IR as well as NR/IR blend is determined according to Equation (1) [38]:

$$L = \frac{m_2 - m_1 \cdot c_F}{m_2} \tag{1}$$

where the mass m_1 corresponds to the rubber compound before extraction. m_2 is the mass of the rubber-filler gel, which is the sum of the undissolvable rubber part and the mass of the filler. c_F is the mass concentration of CB in the single rubber mixture or binary blends. For NR/IR blend the rubber layer $L^{NR/IR}$ is the rubber part in the rubber-filler gel and consists of two contributions according to Equation (2):

$$L^{NR/IR}(t) = L^{NR}(t) + L^{IR}(t) \tag{2}$$

L^{NR} and L^{IR} can be determined using a calibration curve. t is the mixing time. To construct the calibration curve, blends with different NR/IR ratios were prepared and investigated by FTIR according to the procedure described in our previous work [38]. FTIR spectra were recorded by use of an FTIR spectrometer (Bruker Tensor 27, Bruker Corporation, USA) equipped with a diamond attenuated total reflection (ATR) cell. The peaks at 1376 and 888 cm^{-1} were used to calculate the ratio of the surface under the peak (A^{NR}/A^{IR}). The correlation between the A^{NR}/A^{IR} ratio and the given NR/IR mass ratio can be established and based on this correlation the ratio L^{NR}/L^{IR} of the rubber-filler gel can be determined experimentally.

The selective wetting of CB in the NR/IR blend can be calculated according to Equations (3) and (4):

$$\frac{S^{NR}(t)}{S^{IR}(t)} = \frac{L_P^{IR}}{L_P^{NR}} \cdot \frac{L^{NR}(t)}{L^{IR}(t)} \tag{3}$$

$$S^B = S^{NR}(t) + S^{IR}(t) \tag{4}$$

where S^{NR} and S^{IR} are the CB surface fractions wetted by the NR and IR components of the blend, respectively. S^B is the total filler surface fraction wetted in the blend. S^B becomes 1 when CB is completely wetted after 30 min of mixing. L_P^{NR} and L_P^{IR} are the saturated rubber layer in the gel of the single compounds. They can be determined from extraction experiments of the samples at a long mixing time of about 30 min.

2.3. Characterization

Optical microscopy

Optical microscopy (Leica DMRX, Leica Microsystems Inc., Wetzlar Germany) was used to characterize the macrodispersion of the filler. The macrodispersion A/A_0 is calculated by the ratio of the projected area of non-dispersed agglomerates to that of the image. A value A/A_0 = 0% means an image without agglomerates larger than 6 µm.

Transmission electron microscopy (TEM)

Microstructure was examined using a transmission electron microscope (LIBRA 120 MC, Carl Zeiss SMT GmbH, Oberkochen, Germany) with an acceleration voltage of 120 kV. Ultrathin sections (approximately 60 nm) of each sample were prepared at –160 °C with a diamond knife on a cryo-ultramicrotome (Diatome Ltd, Switzerland).

Raman spectroscopy

The Raman spectra were performed using the Raman microscope alpha 300R (WITec GmbH, Ulm, Germany). The excitation laser wavelength was 532 nm, and the laser power was 300 µW. The objective had a magnification of 20×, and the integration time was 500 ms with 500 accumulations. Six measurements were made for each sample. All spectra are baseline corrected and smoothed by the Savitzky–Golay method.

Fourier transform infrared spectroscopy (FTIR)

FTIR analysis (Bruker Tensor 27, Bruker Corporation, USA) equipped with a diamond ATR cell were performed for the gel obtained from extraction experiment of rubber blends. Five spectra were recorded for each sample in the wavenumber range of 4000–700 cm^{-1} with a resolution of 2 cm^{-1}. For NR and DPNR the peak at 1376 cm^{-1} (bending vibration of –CH) and for ENR at 880 cm^{-1} (asymmetric stretching vibration of the epoxy ring) and for IR, the peak at 888 cm^{-1} (bending vibration of $=CH_2$) were used to calculate the ratio of the surface under the peak.

Online measurement of the electrical conductance in the internal mixer

The setup for electrical measurement during the mixing was described in our previous work [39]. A conductivity sensor system was installed in the chamber of the internal mixer to measure the electrical signal of the conductive mixtures.

Rheometer measurement

The torque of fresh single compounds was recorded with a Rheometer (Scarabaeus SIS V-50, Scarabeus GmbH, Germany) at 80 °C to characterize the flocculation of filler.

3. Results and discussion

3.1. Wetting behavior and dispersion of CB and silica in different rubbers

The wetting kinetics of CB in rubber compounds can be described by the rubber layer L in dependence on mixing time (Figure 1a). According to the *infiltration* model proposed by Li *et al*. [40], the wetting of CB by NR, DPNR, ENR and IR molecules and CB dispersion take place simultaneously with increasing mixing time. The rubber layer L of the four rubber compounds investigated increases with different rates and reaches a plateau value after 7 and 9 min for NR, DPNR and ENR and 30 min for IR. According to our previous work [41], the evolution of the rubber layer L can be theoretically calculated by Equation (5):

$$L = \frac{hbt^{1/2}}{hbt^{1/2} + \frac{\rho_F}{\rho_R}(1-\varepsilon)} \tag{5}$$

where ε is the porosity and ρ_F is the density of the filler. ρ_R is the density of rubber. b is a measure for the wetting speed and can be described by Equation (6):

$$b = \frac{\varepsilon}{D_0}\sqrt{\frac{Q\gamma_R \cos\theta}{3\eta_R} + \frac{Q^2\Delta P}{6\eta_R}} \tag{6}$$

where ΔP is the pressure in the mixing chamber, Q is considered as the pore size of the filler. γ_R is the surface tension of rubber, θ is the contact angle and η_R is the rubber viscosity. D_0 is the average agglomerate diameter. The correlation between the plateau value of the rubber layer L_P and the factor h can be described by Equation (7):

$$L_P = \frac{\varepsilon h}{\varepsilon h + \frac{\rho_F}{\rho_R}(1-\varepsilon)} \tag{7}$$

By fitting Equation (5) to the experimental data presented in Figure 1a with ρ_R = 0.94 g/cm^3 and ρ_F = 2.00 g/cm^3, ε = 0.92 [42, 43] the wetting speed b^{NR} = 0.50 $min^{-1/2}$ and b^{DPNR} = 0.44 $min^{-1/2}$, b^{ENR} = 0.44 $min^{-1/2}$ and b^{IR} = 0.25 $min^{-1/2}$ can be experimentally determined for NR, DPNR, ENR and IR, respectively. It is clear that the wetting speed of NR, DPNR and ENR is at a similar level, which is much higher than that of IR. It suggests that the presence

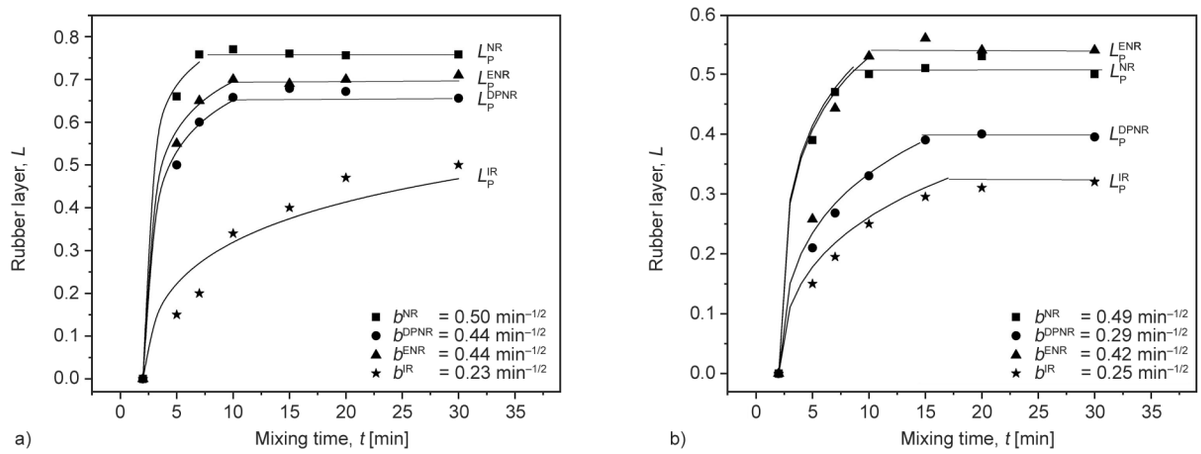

Figure 1. Rubber layer of NR, DPNR, ENR and IR compound filled with CB (a) and silica (b), respectively, in dependence on mixing time.

of the phospholipids in NR, DPNR and ENR may be the main reason for the fast wetting of CB. The small difference between b^{NR}, b^{DPNR} and b^{ENR} could be due to the presence of proteins and epoxy groups. In the absence of the phospholipids, the CB wetting behavior is greatly reduced, as seen in the case of IR.

Figure 1b shows the wetting of silica in four rubbers as a function of mixing time. The wetting speed b^{NR} and b^{ENR} is similar at a level significantly higher than that of b^{DPNR} and b^{IR}. The insignificant difference between b^{DPNR} and b^{IR} might be related to the fact that phospholipids have no effect on the rubber-silica interaction. The high value of b^{ENR} indicates a good rubber-filler interaction between ENR and silica. The interaction between epoxy groups of ENR and silica has been extensively characterized [44, 45]. Using the TEM network visualization technique, Chapman *et al*. [44] found that the voids between silica and rubber are clearly visible for the NR/silica compounds. After epoxidation, the networks of natural rubber epoxidized with 25 and 50 mol% (ENR25 and ENR50) are fully bound to thesilica particles and no voids are seen, indicating a higher rubber-silica affinity for the ENR/silica compounds. Based on the results made by different test methods, Luo *et al*. [45] confirm that hydrogen bonding exists between the epoxy rings of ENR and silanols of silica.

The high value of b^{NR} could be due to the presence of proteins. It is well-known that proteins in NR play an important role in controlling NR properties. Proteins in NR have significantly affected the vulcanization characteristics, dynamic and mechanical properties of NR [46]. Sarkawi *et al*. [12] investigated the rubber/silica interphase of NR blends with different protein content using the TEM network visualization technique to gain further insight into the reinforcement mechanism of silica in NR. The physical interaction between silica and proteins through hydrogen bonding with functional protein groups was demonstrated.

However, the higher value of b^{NR} compared to b^{ENR} does not allow the conclusion that the NR-silica interaction is stronger than that of ENR and silica. According to Equation (6) the wetting speed b is determined, among other things, by the rubber viscosity. The strong molecular interaction due to epoxy groups of ENR and, thus, the high viscosity may be the reason for the slower wetting of ENR compared to NR.

Roughly speaking, the better the interaction between rubber and filler, the better the dispersion of the filler. The optical microscopic images of CB-filled rubber compounds are shown in Figure 2a–2d. The dispersion A/A_0 was calculated to quantify the dispersion state of the rubber compound and is shown on the images. The dispersion A/A_0 of CB in NR, DPNR and ENR compounds ranges from 1.5 to 3.2%, which is much better than that of IR compounds. Some CB agglomerates are still visible on the image of the IR compound, and a dispersion A/A_0 of 10.7% was determined. Again, the influence of phospholipids on the improvement of the CB dispersion in NR, DPNR and ENR can be seen, while the effect of proteins and epoxy groups could not be detected. It is obvious that the dispersion state is well correlated with the wetting speed b shown in Figure 1a.

The dispersion of silica in rubbers used is shown in Figure 2e–2h. The silica dispersion A/A_0 in NR and ENR is 2.1 and 2.7%, respectively, indicating good rubber-filler interaction due to the presence of proteins and epoxy groups, as discussed in Figure 1b. The

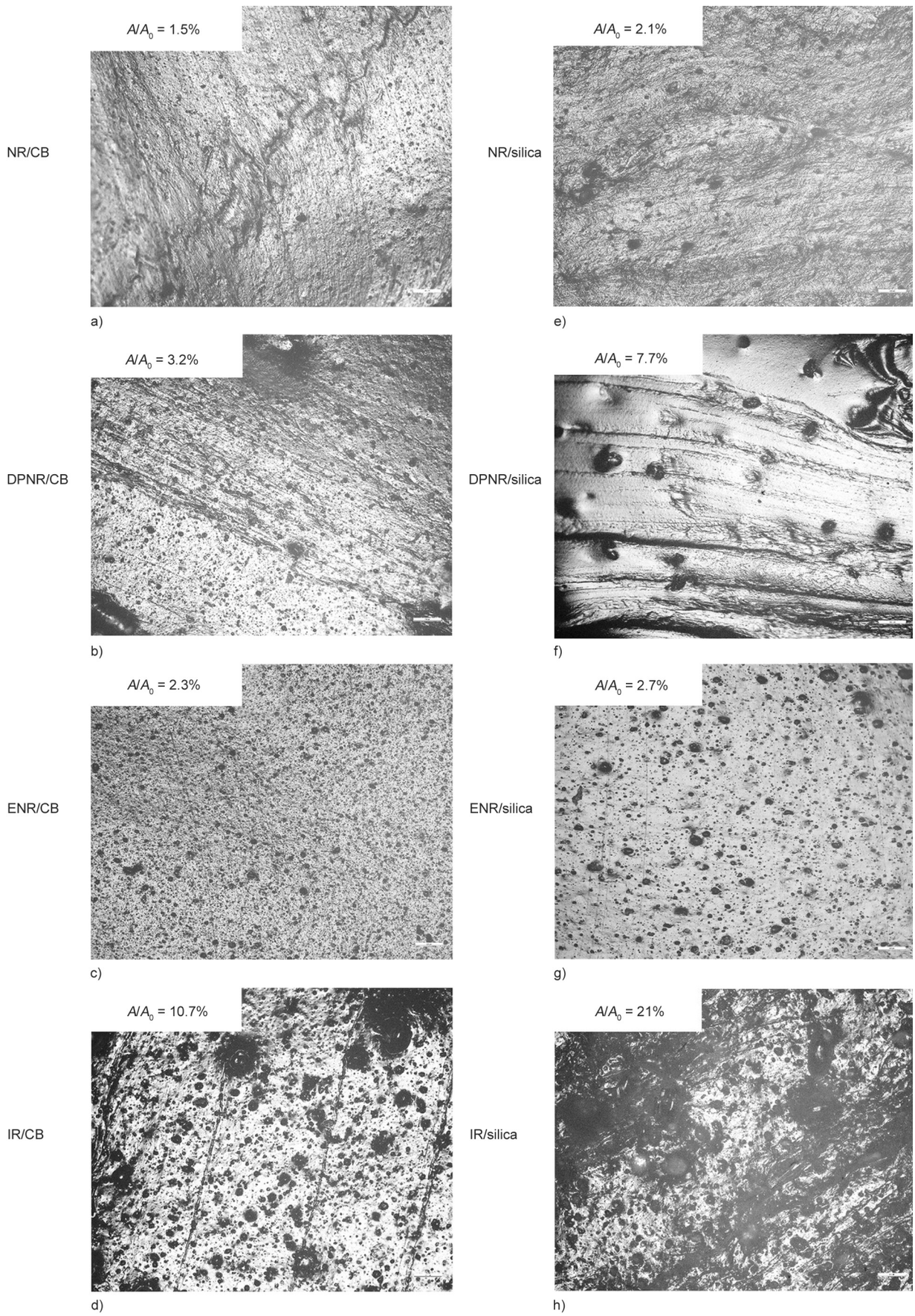

Figure 2. Optical microscopic images (1100 μm×700 μm) of NR, DPNR, ENR, and IR compounds filled with CB and silica, respectively, taken at 30 min mixing time: a) NR/CB, b) DPNR/CB, c) ENR/CB, d) IR/CB, e) NR/silica, f) DPNR/silica, g) ENR/silica, h) IR/silica.

lower wetting speed of silica by DPNR and IR observed in Figure 1b due to poor rubber-filler interaction results in poor dispersion of silica in Figures 2f and 2h, respectively. It is worth noting that b^{DPNR} of 7.7% is much lower than b^{IR} of 21%. However, at this stage, it is not clear whether the phospholipids in DPNR positively affect the dispersion process and whether the interaction between DPNR and silica is stronger than that of IR and silica.

From Figures 1 and 2, it can be seen that phospholipids significantly support the interaction between NR and CB. It can be assumed that the cation of phospholipids can interact with the π-π electrons on the graphite-like surface of CB. Kreyenschulte *et al*. [17] reported that Raman spectroscopy was used to characterize the state of aggregation of carbon black in ionic liquid and polymer matrix. Raman studies have shown that the ionic liquid accumulates preferentially at the edges of the graphitic crystals through cation-π interactions due to the highest adsorption energies. This effect is even more pronounced when the carbon black is graphitized and thus a larger fraction of the carbon black surface is covered with graphitic crystals. These strong cation-π-interactions also cause a shift of the D- and the G-band to higher wavenumbers.

In the present work, the Raman spectra of four CB-filled rubber compounds show typical D and G peaks corresponding to the presence of sp^3 defects and vibration of sp^2 carbon atoms in the CB surface, respectively. The shift of the D-band and G-band and the change of the D/G ratio were determined in order to estimate the interaction between phospholipids and CB. Table 6 shows the positions of the D-band and G-band and the D/G ratio of all mixtures compared with those of the as-received CB. The D-band and G-band of as received CB are determined at 1336 and 1589 cm^{-1}, and shift slightly to about 1345 and 1601 cm^{-1} for CB filled compounds. The D/G ratio of the CB-filled compounds is about 1.32, which is slightly higher than that of the as received CB of 1.29. Because of the slight red shift of the D-band and G-band and the slight change of D/G ratio, it is difficult to discuss the interaction between the rubber and CB. The effect of functional groups like phospholipids, protein and epoxy groups in NR on the rubber-CB interaction could not be observed by Raman investigation in the present study. This could be related to the fact that the concentration of the non-rubber components of NR is below a critical concentration [47].

Table 6. Results from Raman investigation: D-band, G-band, and D/G ratio.

Sample	D-band	G-band	D/G ratio
CB	1336	1589	1.29
NR/CB	1344	1600	1.33
DPNR/CB	1347	1603	1.35
ENR/CB	1346	1601	1.32
IR/CB	1345	1601	1.32

3.2. New test strategy: selective wetting of filler in NR/IR, DPNR/IR and NR/ENR blends

To directly compare the rubber-filler affinity of CB or silica with different rubbers, CB or silica was added to 50/50 NR/IR, DPNR/IR and NR/ENR blends. The preferential wetting of the filler surface by a blend component may be a measure of the better rubber-filler interaction of filler with that rubber. The role of the individual functional groups can be determined using this test strategy. Usually, the morphology of filled rubber blends and the phase selective localization of filler in rubber blends can be visualized and characterized by electron microscopy. In Figure 3, TEM images of CB-filled DPNR/IR, NR/IR and NR/ENR blends are shown. Conductive CB is visible as transparent domains because only the outer shell is visible, while the inner part of CB particles is empty [48]. Due to the similarity of the main chain of the blend components and the low contrast between them, it is not possible to observe the selective localization of CB in the studied rubber blends. For the quantification of the phase selective wetting of filler in rubber blends, the *Z-model* and the *wetting concept* developed in our previous work [41] were used.

The prediction of the phase selective filler wetting in a thermodynamic equilibrium state can be made using the *Z-model*, *e.g*. CB in NR/IR blend, using Equations (8) and (9) [41]:

$$\frac{S_{eq}^{NR}}{S_{eq}^{IR}} = n_{NR/IR}\left(\frac{\gamma_{IR}+\gamma_F-2\sqrt{\gamma_{IR}\gamma_F}}{\gamma_{NR}+\gamma_F-2\sqrt{\gamma_{MR}\gamma_F}}\right)^2 \tag{8}$$

$$S_{eq}^{NR}+S_{eq}^{IR}=1 \tag{9}$$

where S_{eq}^{NR} and S_{eq}^{IR} are the filler surface fractions wetted by NR and IR phase in the equilibrium state. $n_{NR/IR}$ is the mass ratio of the rubber phase NR to IR.

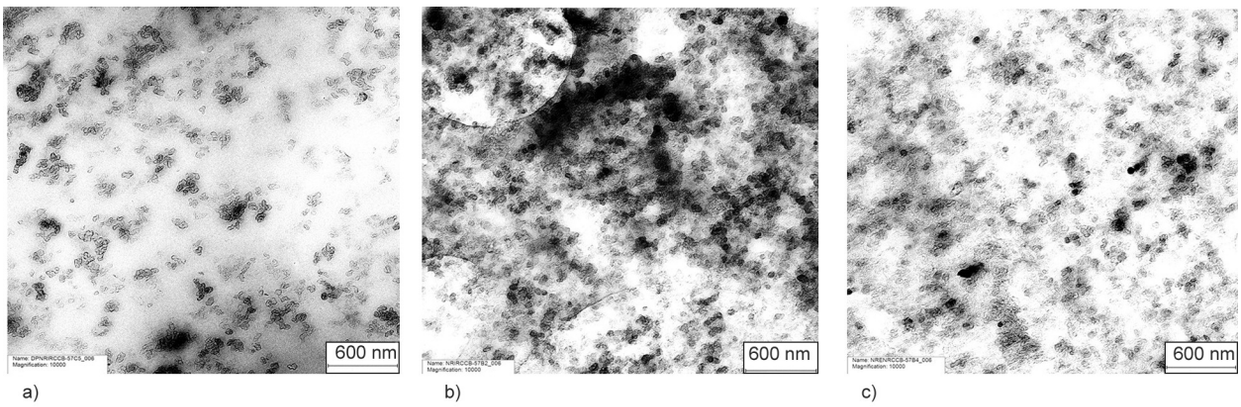

Figure 3. TEM image of DPNR/IR blend filled with 3 phr CB (a); NR/IR blend filled with 10 phr CB (b) and NR/ENR blend filled with 10 phr CB (c).

γ_{NR}, γ_{IR} and γ_F are the surface tension values of the blend components and filler, respectively. If the surface tension values γ_{NR} = 22 mN/m and γ_{IR} = 20 mN/m of rubber components are substituted into Equations (8) and (9) with $n_{NR/IR}$ = 1 for 50/50 NR/IR blend, a Z-shaped master curve is obtained, demonstrating the filler surface fraction wetted by NR phase as a function of the filler surface tension (Figure 4a). Fitting the CB surface tension γ_F = 28 mN/m to the master curve, a CB surface fraction wetted by each phase, S_{eq}^{NR} = 0.79 and S_{eq}^{IR} = 0.21, respectively, can be predicted for a thermodynamic equilibrium state. Similarly, by inserting the silica surface tension γ_F = 72 mN/m into the master curve, a silica surface fraction wetted by each phase, S_{eq}^{NR} = 0.56 and S_{eq}^{IR} = 0.44, respectively, can be predicted. The prediction of CB and silica wetting in other blends was performed as shown in Figures 4b and 4c, respectively. The selective wetting of CB and silica in different blends is summarized in Figure 4d–4f.

The selective wetting of CB and silica in rubber blends can be quantified experimentally using the *wetting concept*. For the creation of the calibration curve, a series of NR/IR blends with different mass ratios was prepared and characterized by FTIR. For example, an FTIR spectrum of 50/50 NR/IR blend is presented in Figure 5a. The peaks at 1376 and 888 cm^{-1} were selected for the characterization of the NR and IR phases, respectively. The correlation between the ratio of the area under the peak A^{NR}/A^{IR} and the given mass ratio NR/IR shown in Figure 5b is described by a straight line. The ratio L^{NR}/L^{IR} needed for Equation (3) can be determined manually using the calibration curve (Figure 5b).

The selective wetting of CB in NR/IR and DPNR/IR blends is shown in Figure 6a as a function of mixing

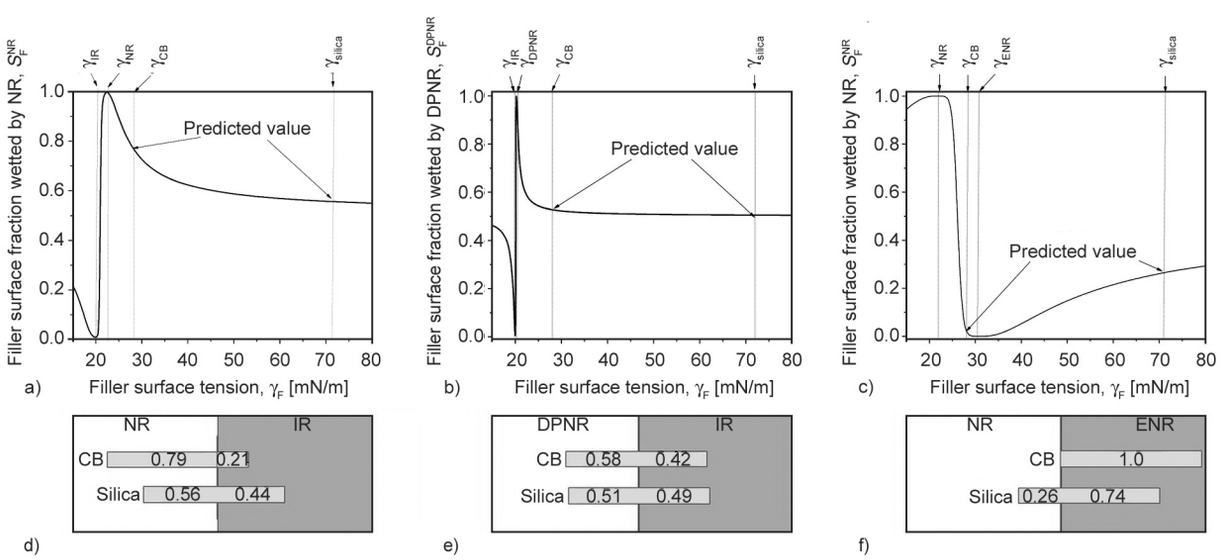

Figure 4. Prediction of selective filler wetting using the *Z-model* for NR/IR (a), (d), DPNR/IR (b), (e) and NR/ENR (c), (f) blend.

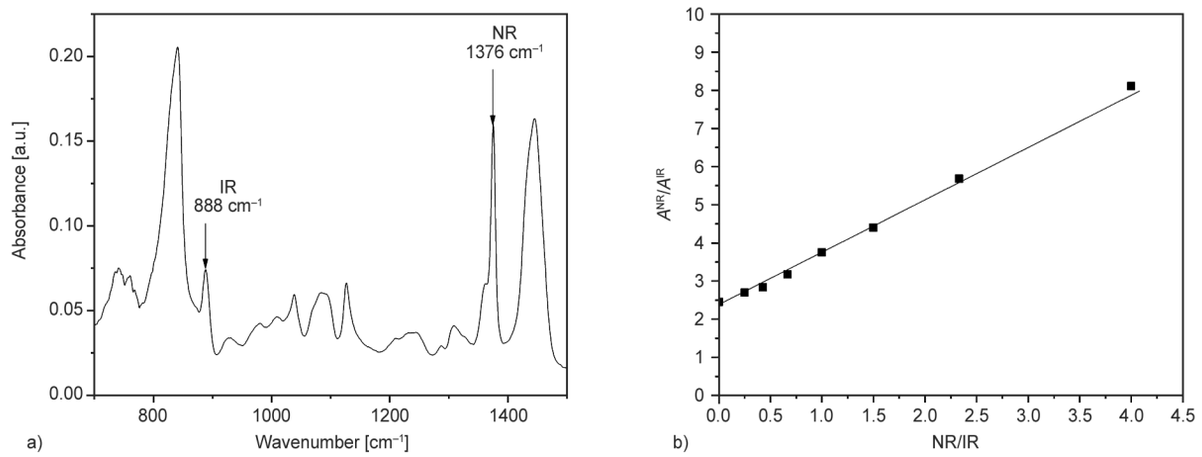

Figure 5. FTIR spectra (a) of NR/IR blend and calibration curve (b).

time. It is clear that the surface of CB is thoroughly wetted by the NR phase immediately after the addition of CB to the blend. Obviously, deproteinization has no influence on the affinity of natural rubber for CB. Therefore, it can be concluded that phospholipids are essential for the rubber-filler interaction of CB in NR. When CB is mixed in NR, the ammonium cation N^+ of phospholipids can interact with the CB surface via cation interaction and form stable bonds in addition to van der Waals bonds. Cation-π interaction was proposed by Ma and Dougherty [49] Fukushima and Aida [50] as the main linkage for CNTs and ionic liquid and by Kreyenschulte *et al*. [17] for conductive CB and ionic liquid. Narongthong *et al*. [51] investigated the interactions between 1-allyl-3-methyl-imidazolium chloride (AMIMCl) and conductive carbon black in rubber compounds. They found that the presence of cation-π interactions between the cations of the AMIMCl and the π-electrons of the graphitic structures at the carbon black surface can have a considerable effect on the final properties of elastomer composites. Brennan *et al*. [52] found that the production or the heat treatment at higher temperatures could transfer amorphous CB to graphitic crystal; thus, the extent of active π-π electrons is increased. The strong cation-π interaction

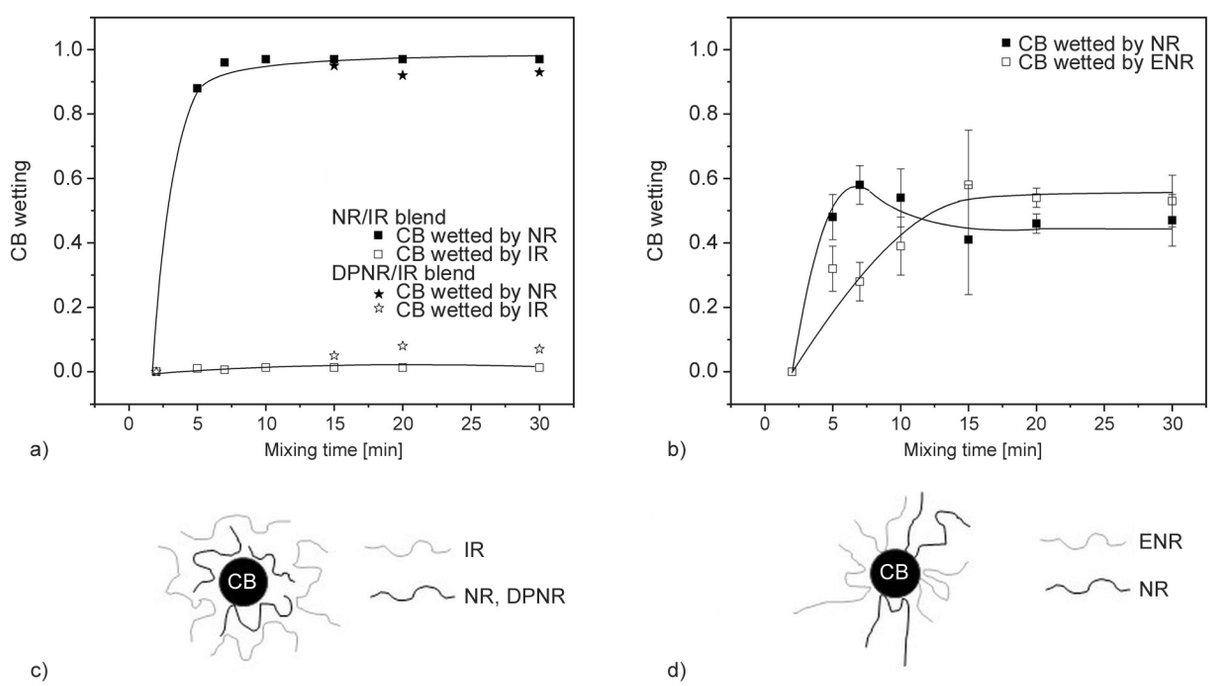

Figure 6. Selective CB wetting in NR/IR and DPNR/IR (a) and NR/ENR blend (b) in dependence on mixing time; Illustration of CB wetting by different rubbers (c), (d).

leads to the formation of a filled structure with a CB core and an inner shell of NR or DPNR and an outer layer of IR, as illustrated in Figure 6c.

When CB was mixed into NR/ENR blend, the CB surface fraction S_F^{NR} increased faster than S_F^{ENR} in the first mixing stage up to 7 min mixing time, which could correlate with the faster wetting speed b^{NR} compared to b^{ENR}, as shown in Figure 1a. After 7 minutes, SFNR decreases slightly, while SFENR increases until a plateau is reached. NR and ENR can be expected to simultaneously wet CB in the initial mixing period up to 7 min of mixing time, but about 60% of CB surface is wetted by NR because of the faster b^{NR}. Phospholipids in NR and ENR act as anchor points that firmly connect the NR and ENR ends to the CB surface. The presence of epoxy groups in ENR can enhance its interaction with CB through van der Waal bonds between its backbone and CB surface, as shown in Figure 6d. Through their conformational rearrangement and thermodynamic driving forces, ENR molecules partly replace NR molecules on the CB surface in the second period from 7 min to 30 min mixing time (Figure 6b).

The selective wetting of silica in the NR/IR blend is presented in Figure 7a. NR wets silica faster than IR and at the end of the mixing S_F^{NR} reaches a value of 0.54, while S_F^{IR} is 0.46. The slightly higher value of S_F^{NR} might indicate the small contribution of proteins to the NR-silica interaction. DPNR and IR show the same wetting behavior towards silica in Figure 7b, which means that phospholipids have no influence on the interaction between NR and silica. According to the results reported in the literature [12, 46], the physical interaction between silica and proteins may enhance NR-silica interaction through hydrogen bonding with functional protein groups. However, according to our results, this enhancement is not strong enough to help NR displace IR molecules from the silica surface. Thus, both blend components are found on the surface of silica in NR/IR, and DPNR/IR blends, as illustrated in Figures 7d and 7e. A direct comparison of silica wetting in NR/IR and DPNR/IR blends allows us to evaluate the effectiveness of the protein-silica interaction. In this case, the protein-silica interaction is negligible, and the rubber-silica interaction in NR, DPNR, and IR compounds is mainly determined by the van der Waals bonding between the isoprene backbone and silica surface.

Figure 7c shows the wetting of silica in the NR/ENR blend. In the first mixing period of up to 7 min, silica is wetted faster by NR than by ENR. That is due to the higher wetting speed b^{NR} compared to b^{ENR}, as discussed in Figure 1b. In the second mixing period, after 7 min, ENR molecules gradually replace part of NR molecules on the silica surface. This result is related to the higher affinity of silica to ENR than to NR. At a mixing time of 30 minutes, a silica surface fraction of 0.23 is wetted by NR, while ENR wets a surface fraction of 0.77. The stronger ENR/silica interaction compared to NR/silica may be due to both (1) a stronger interaction between epoxy groups and silica and (2) the fact that epoxy groups in ENR are much more numerous (50 mol%) than proteins in NR (6 wt%). According to Sarkawi *et al*. [12], although proteins are able to interact with the silica surface and reduce the filler-filler interaction, they do not contribute to strong rubber-filler interactions, as the silica-protein interaction only leads to the formation of physically bound rubber.

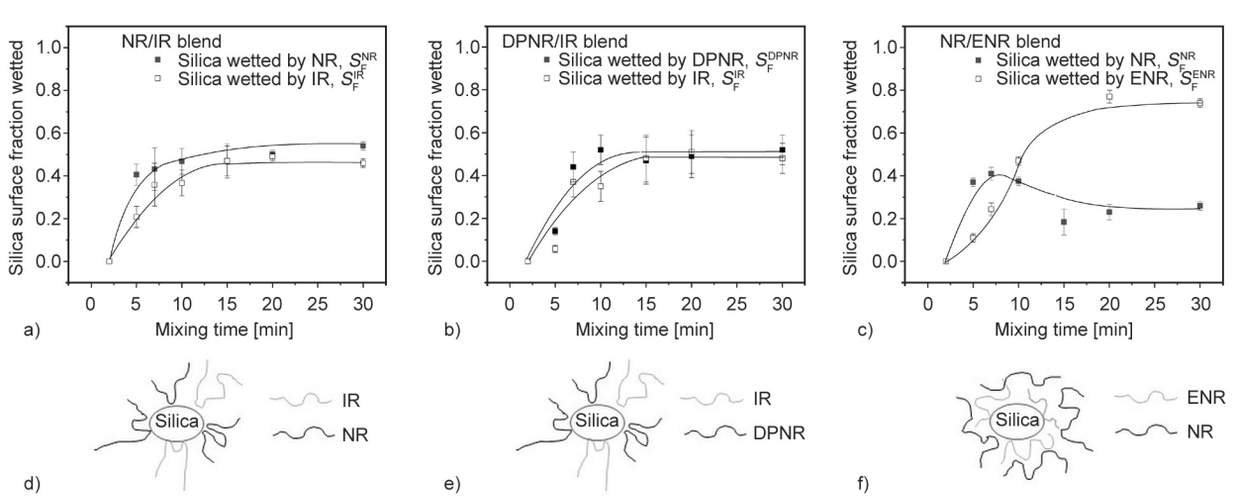

Figure 7. Selective wetting of silica in NR/IR (a), (d), DPNR/IR (b), (e) and NR/ENR (c), (f) blend.

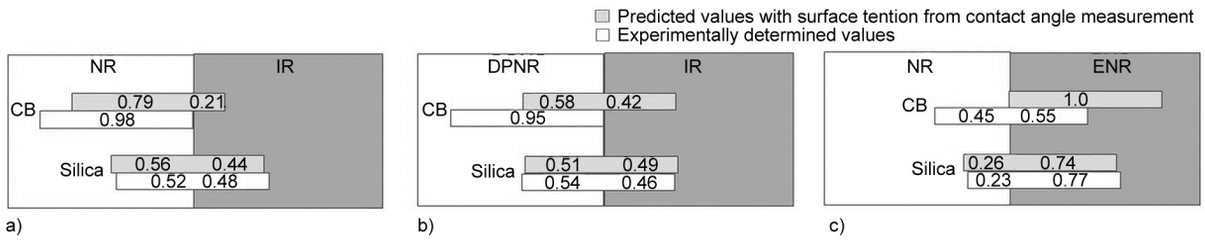

Figure 8. Comparison between prediction and experimental determination of selective wetting of CB and silica in different rubber blends:a) NR/IR, b) DPNR/IR and c) NR/ENR blend.

The experimentally determined selective wetting of CB and silica is shown in Figure 8 in comparison with the wetting predicted by the *Z-model*. It is interesting to observe that the experimentally determined values for the silica-filled blends agree well with the predicted values. It is worth mentioning that the surface tension values used for the prediction were obtained by contact angle measurements, which are characteristic of the entire main chains of the rubber and silica surface. The very good agreement between the predicted selective wetting and the experimentally determined values indicates that the interaction between rubber and silica is mainly determined by the physical affinity between the rubber main chains and the silica surface. The presence of epoxy groups along the ENR molecules increases the surface tension from 22 to 30.6 mN/m and decreases the difference between the surface tension of ENR and silica. This is the reason for the preferential wetting of silica by ENR. As can be seen in Figures 7a and 7b, phospholipids and proteins have no influence on the interaction between NR and silica since they are present at the end of the rubber molecules and only in small amounts.

In contrast to silica wetting, the prediction of CB wetting does not agree with the experimentally determined values for all three mixtures, as shown in Figure 8. As explained in Figure 6, the strong affinity between NR and CB is caused by the phospholipids via the cation-π bonds. The disagreement with the prediction may be related to the fact that the contact angle measurement determined the surface tension value of NR used for prediction. Since the content of the phospholipids is very low (<1.0 wt%) and they are bound to the end of NR, they cannot migrate to the surface of the rubber sample. Therefore, the surface tension is determined merely by the isoprene backbone and does not reflect the role of phospholipids.

To quantify the effect of phospholipids on the CB wetting in the NR/IR blend, the surface tension value of NR is gradually increased while the surface tension of IR and CB is kept constant. The obtained master curve changes accordingly in the direction indicated by the arrow in Figure 9a. When the predicted S_{eq}^{NR} reaches the experimentally determined value S_F^{NR} of 0.95, the surface tension of NR reaches the value of 26.5 mN/m. Thus, the effect of phospholipids on the NR-CB interaction can be quantitatively described by the corrected value of the surface tension of NR, $corr\gamma_{NR}$ = 26.5 mN/m, which agrees well with the values obtained for other systems [34]. The same procedure was performed to determine the corrected surface tension of DPNR and ENR, and we obtained

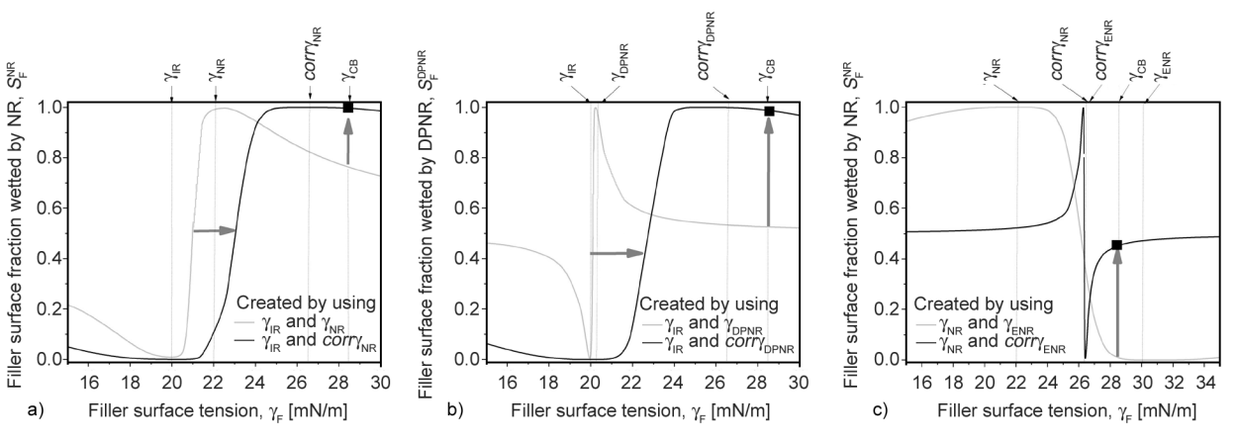

Figure 9. Master curve of filler wetting in NR/IR (a), DPNR/IR (b), and NR/ENR (c) blend observed by changing the surface tension of NR, DPNR, and ENR, respectively.

$corr\gamma_{DPNR}$ = 25.9 mN/m and $corr\gamma_{ENR}$ = 26.2 mN/m, as shown in Figures 9b and 9c, respectively.

3.3. Verification of the results received by the new test strategy

3.3.1. Rubber-filler interaction and filler flocculation

It has been demonstrated that when the filler is well dispersed in the polymer, the aggregates tend to re-agglomerate during storage and vulcanization of the uncured compound, especially at high filler loading [53]. Accordingly, the formation of filler networks in the polymer matrix is mainly determined by the attractive force between filler aggregates and the interaction between polymer molecules, as well as the interaction between filler and polymer. Wang [53] proposed a model to predict the tendency of filler agglomeration in a filled compound. According to this model, when two filler particles agglomerate, a pair of filler particles and a pair of polymer units are formed. In this process, the change in potential energy is considered as the driving force for filler agglomeration. The change in potential energy ΔW can be estimated from the total change in adhesion energy in the agglomeration process. The higher ΔW is, the stronger the filler flocculation. The change in potential energy ΔW is given by Equation (10):

$$\Delta W = 2\left(\sqrt{\gamma_R^d} - \sqrt{\gamma_F^d}\right)^2 + 2\left(\sqrt{\gamma_R^p} - \sqrt{\gamma_F^p}\right)^2 + \\ + 2\left(W_R^x + W_F^x - 2W_{RF}^x\right) \quad (10)$$

where γ_R^d and γ_R^p are the dispersive and polar components of the surface energy of the rubber, respectively. γ_F^d and γ_F^p are the dispersive and polar components of the surface energy of the filler, respectively. W_R^x and W_F^x are the cohesion work comprising of different types of cohesive forces, such as dispersive, dipole-dipole, induced dipole-dipole, acid-base, and hydrogen bonding in rubber and filler. W_{RF}^x is the adhesion work that originated from different types of molecular interactions between rubber and filler. Generally, for hydrocarbon polymers filled with conventional fillers like CB and silica, the terms W_R^x, W_F^x and W_{RF}^x iare considered negligible [53, 54]. Assuming that they can be negligible for the systems investigated, the change in adhesion energy ΔW can be calculated. As an example, the tendency for flocculation of CB and silica in NR and IR was predicted using Wang's model. Setting the values of surface energy given in Table 7, we observed $\Delta W_{NR\text{-}CB}$ = 15.38 mN/m for NR/CB compound and $\Delta W_{IR\text{-}CNT}$ = 11.38 mN/m for IR/CB compound as well as $\Delta W_{NR\text{-}silica}$ = 47.6 mN/m for NR/silica compound and $\Delta W_{IR\text{-}silica}$ = 57.3 mN/m for IR/silica compound. Based on this result, the tendency of flocculation of CB in NR would be stronger than in IR, and that of silica in NR would be weaker than in IR.

The flocculation of CB in rubber compounds can experimentally be characterized by monitoring the development of the online electrical conductance and torque at 80 °C, respectively, as presented in Figures 10a and 10b. It is obvious that the online conductance and the torque of the IR/CB compound increase sharply compared to the other rubber compounds, which is due to the strong flocculation process of CB in the IR compound. This behavior corresponds very well with the poor IR-CB interaction

Table 7. Prediction of the tendency of flocculation of CB and silica in NR and IR compounds, respectively, according to Wang's model.

Filled compound	γ^d [mN/m]	γ^p [mN/m]	$\Delta W_{rubber\text{-}CB}$ [mN/m]	$\Delta W_{rubber\text{-}silica}$ [mN/m]
NR	16	6	15.38	47.6
IR	16	4	11.38	57.3
CB	28	0		
Silica	17	58		

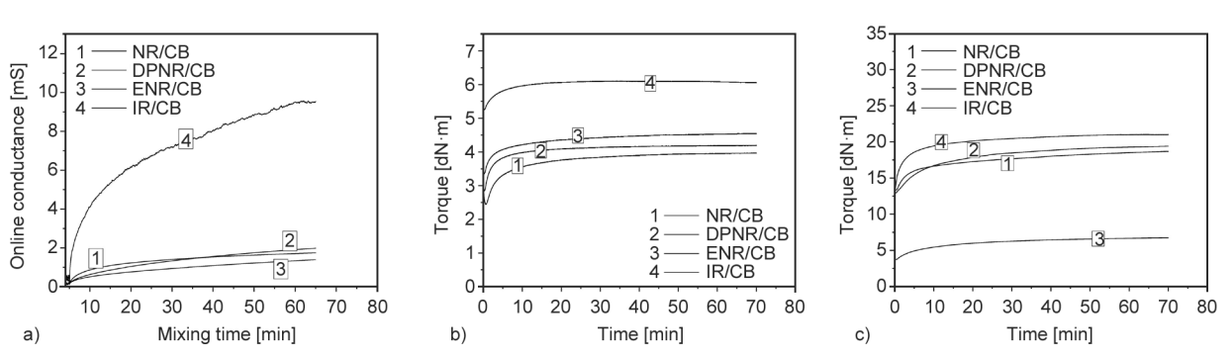

Figure 10. Online conductance-time characteristics (a) of CB-filled compounds and torque-time characteristics, (b), (c) of compounds filled with CB and silica, respectively, at 80 °C.

shown in Figure 6. Due to the presence of phospholipids, NR, DPNR, and ENR strongly interact with the CB surface, resulting in a low flocculation tendency of CB, as reflected by the low development of the online conductance and the torque in Figures 10a and 10b, respectively. The experimental result shown in Figures 10a and 10b, where the flocculation of CB in IR is considerably pronounced, are obviously in contradiction with the prediction made by Equation (10). That is related to the fact that the value of surface energy of NR used for prediction does not consider the influence of phospholipids on the rubber-filler interaction.

NR/silica and DPNR/silica, as well as IR/silica compounds, show pronounced flocculation of the silica, as shown by the increase in torque in Figure 10c, while only insignificant flocculation is observed for ENR/silica compounds. This agrees well with our result on silica wetting in Figure 7. A closer look at curves 1 and 4 in Figure 10c shows that silica flocculation is somewhat more pronounced in the IR compound than in the NR compound, which was well predicted by Wang's model.

3.3.2. Prediction of selective wetting of hybrid filler CB/silica in rubber blends using the corrected surface tension

In our previous work [26] a BIIR/NR blend filled with hybrid filler CB/silica was prepared to develop a self-healable composite. The selective wetting of CB and silica in the blend was quantified by our new method and correlated well with the self-healing properties of the sample. In the present work, the selective wetting of hybrid filler CB/silica in BIIR/NR, BIIR/DPNR, BIIR/ENR and BIIR/IR blends was predicted by means of the *Z-model*. The corrected surface tension of NR, DPNR and ENR was considered for the prediction of CB wetting,

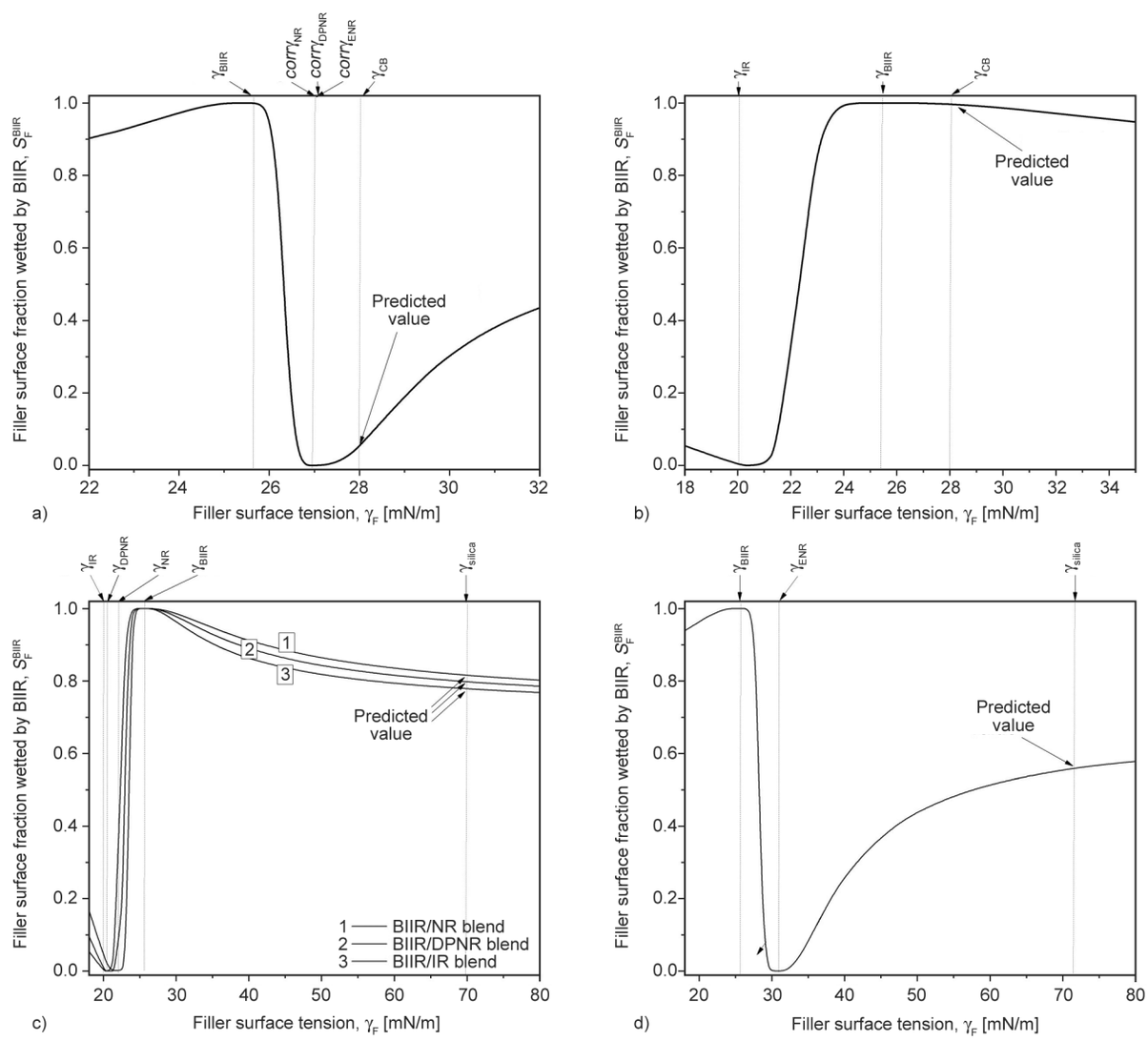

Figure 11. Prediction of selective wetting of CB (a, b) and silica (c, d) in different BIIR blends.

as shown in Figure 11a. Figure 11b shows the master curve for predicting CB wetting in the BIIR/IR blend. The silica wetting in BIIR/NR, BIIR/DPNR, and BIIR/IR blend is predicted in Figure 11c. The prediction of silica wetting in the BIIR/ENR blend is shown in Figure 11d.

TEM images of BIIR/NR, BIIR/DPNR, BIIR/ENR, and BIIR/IR blends are shown in Figure 12. The predicted values of CB and silica wetting are shown in the right side of TEM images for comparison. It is clear that CB domains are mainly found in the NR, DPNR, and ENR phases of the

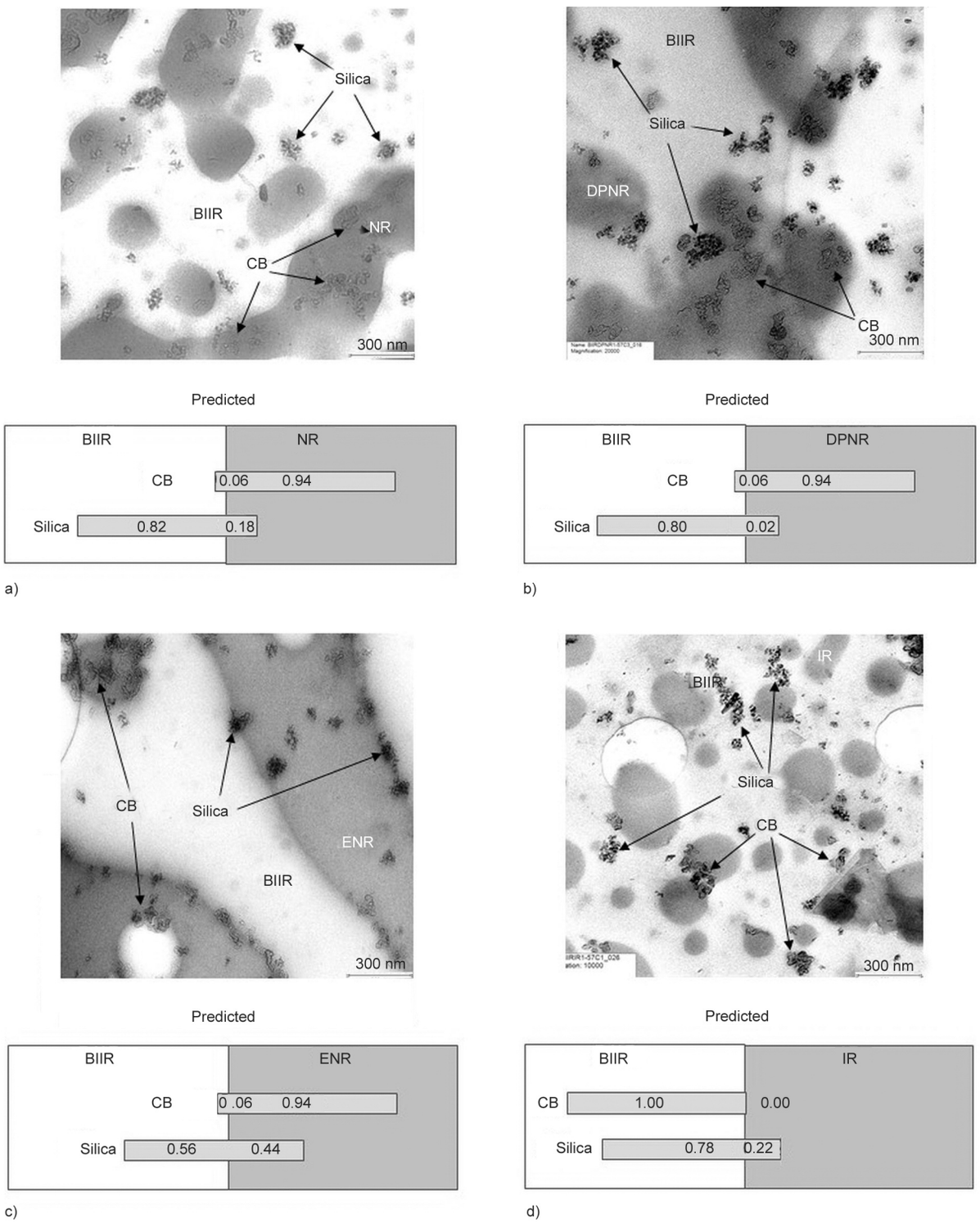

Figure 12. TEM images of BIIR/NR (a), BIIR/DPNR (b), BIIR/ENR (c) and BIIR/IR (d) blend filled with hybrid filler CB/silica.

BIIR blend, respectively (Figure 12a–12c). In BIIR/IR blend, no CB domains are observed in the IR phase due to the absence of phospholipids (Figure 12d). Silica domains are mainly seen in the BIIR phase of BIIR/NR, BIIR/DPNR, and BIIR/IR blend since the NR-silica, DPNR-silica, and IR-silica interactions are poor compared to the BIIR-silica interaction. Epoxidation of NR improves the ENR-silica interaction, thus forcing some of the silica to migrate to the ENR phase, as shown in Figure 12c. In general, morphological characterization of CB and silica wetting by TEM can qualitatively support the prediction shown on the right side of the images.

4. Conclusions

A new test strategy has been proposed to characterize the effect of functional groups on the interaction between rubber and filler in a rubber compound. In principle, the filler is mixed into a blend of rubber A and rubber B that is made by functionalizing rubber A with a specific chemical group. The phase-selective wetting of the filler is directly related to the effect of the functional group. Based on the new test strategy, the effect of the non-rubber components in NR and their epoxidation on the rubber-filler interaction in CB-filled NR compounds was investigated. Accordingly, CB was blended in three blends consisting of NR/isoprene (IR), deproteinized natural rubber (DPNR)/IR, and NR/epoxidized NR (ENR). The phase-selective wetting of CB by different rubber molecules was quantitatively characterized using the *wetting concept*. Based on the selective wetting of the filler, the rubber-filler affinity can be discussed, and the role of non-rubber components and epoxy groups can be distinguished. It was found that proteins and epoxide groups do not affect the affinity between NR and CB, while the linked phospholipids interact with the CB surface through cation-π bonding. By fitting the experimentally determined selective wetting of CB into the *Z-model*, a corrected surface tension of CB describing the effect of phospholipids was determined. The proposed test strategy was used for silica as a reference filler. It was found that epoxy groups are essential for the strong interaction between ENR and silica, while proteins show a weak interaction and phospholipids have no effect. The proposed test strategy was used for other rubber blends containing hybrid filler CB/silica as reference fillers to demonstrate the transferability and verification of the method. In addition, the new test strategy can be used to characterize the selective wetting of different fillers in blends of miscible rubber components. It opens up a new possibility for a direct comparison of two similar and/or miscible rubbers with respect to their rubber-filler interactions.

Acknowledgements

The authors thank the German Research Foundation (DFG project Nr. 417949845) for the financial support.

References

[1] Kang M-J., Heo Y-J., Jin F-L., Park S-J.: A review: Role of interfacial adhesion between carbon blacks and elastomeric materials. Carbon Letters, **18**, 1–10 (2016). https://doi.org/10.5714/CL.2016.18.001

[2] Dannenberg E. M.: Bound rubber and carbon black reinforcement. Rubber Chemistry and Technology, **59**, 512–524 (1986). https://doi.org/10.5254/1.3538213

[3] Robertson C. G., Hardman N. J.: Nature of carbon black reinforcement of rubber: Perspective on the original polymer nanocomposite. Polymers, **13**, 538 (2021). https://doi.org/10.3390/polym13040538

[4] Tunnicliffe L. B., Kadlcak J., Morris M. D., Shi Y., Thomas A. G., Busfield J. J. C.: Flocculation and viscoelastic behaviour in carbon black-filled natural rubber. Macromolecular Materials Engineering, **299**, 1474–1483 (2015). https://doi.org/10.1002/mame.201400117

[5] Gabriel D., Karbach A., Drechsler D., Gutmann J., Graf K., Kheirandish S.: Bound rubber morphology and loss tangent properties of carbon-black-filled rubber compounds. Colloid Polymer Science, **294**, 501–511 (2016). https://doi.org/10.1007/s00396-015-3802-6

[6] Han S., Kim W-S., Mun D-Y., Ahn B., Kim W.: Effect of coupling agents on the vulcanizate structure of carbon black filled natural rubber. Composite Interfaces, **27**, 355–370 (2019). https://doi.org/10.1080/09276440.2019.1637197

[7] Ghosh A. K., Maiti S., Adhikari B., Ray G. S., Mustafi S. K.: Effect of modified carbon black on the properties of natural rubber vulcanizate. Journal of Applied Polymer Science, **66**, 683–693 (1997). https://doi.org/10.1002/(SICI)1097-4628(19971024)66:4<683::AID-APP8>3.0.CO;2-O

[8] Salaeh S., Nakason C.: Influence of modified natural rubber and structure of carbon black on properties of natural rubber compounds. Polymer composites, **33**, 489–500 (2012). https://doi.org/10.1002/pc.22169

[9] Park S-J., Cho K-S., Ryu S.: Filler–elastomer interactions: Influence of oxygen plasma treatment on surface and mechanical properties of carbon black/rubber composites. Carbon, **41**, 1437–1442 (2003). https://doi.org/10.1016/S0008-6223(03)00088-5

[10] Park S-J., Kim J-S.: Modifications produced by electrochemical treatments on carbon blacks: Microstructures and mechanical interfacial properties. Carbon, **39**, 2011–2016 (2001). https://doi.org/10.1016/S0008-6223(01)00015-X

[11] Schröder A., Klüppel M., Schuster R. H.: Characterisation of surface activity of carbon black and its relation to polymer-filler interaction. Macromolecular Materials and Engineering, **292**, 885–916 (2007). https://doi.org/10.1002/mame.200700032

[12] Sarkawi S. S., Dirkes W. K., Noodermeer J. W. M.: Elucidation of filler-to-filler and filler-to-rubber interactions in silica-reinforced natural rubber by TEM network visualization. European Polymer Journal, **54**, 118–127 (2014). https://doi.org/10.1016/j.eurpolymj.2014.02.015

[13] Sato Y. K., Kuwauchi Y., Miyoshi W., Jinnai H.: Visualization of chemical bonding in a silica-filled rubber nanocomposite using STEM-EELS. Scientific Reports, **10**, 21558 (2020). https://doi.org/10.1038/s41598-020-78393-0

[14] Ma J-H., Zhang L-Q., Wu Y-P.: Characterization of filler-rubber interaction, filler network structure, and their effects on viscoelasticity for styrene-butadiene rubber filled with different fillers. Journal of Macromolecular Science Part B: Physics, **52**, 1128–1141 (2013). https://doi.org/10.1080/00222348.2012.755441

[15] Gengadhar J., Maheshwari A., Bordia R. K., Kumar C. N. S., Kubel C., Sujith R.: Role of carbon on the thermal and electrical properties of graphene- enriched silicon oxycarbides. Ceramics International, **46**, 28156–28164 (2020). https://doi.org/10.1016/j.ceramint.2020.07.314

[16] Salvi A. M., Pucciariello R., Guascito M. R., Villani V., Intermite L.: Characterization of the interface in rubber/silica composite materials. Surface and Interface Analysis, **33**, 850–861 (2002). https://doi.org/10.1002/sia.1463

[17] Kreyenschulte H., Richter S., Götze T., Fischer D., Steinhauser D., Klüppel M., Heinrich G.: Interaction of + and its influence on carbon black filled rubbers. Carbon, **50**, 3649–3658 (2012). https://doi.org/10.1016/j.carbon.2012.03.037

[18] Pantea D., Darmstadt H., Kaliaguine S., Roy C.: Electrical conductivity of conductive carbon blacks: Influence of surface chemistry and topology. Applied Surface Science, **217**, 181–193 (2003). https://doi.org/10.1016/S0169-4332(03)00550-6

[19] Plagge J., Lang A.: Filler-polymer interaction investigated using graphitized carbon blacks: Another attempt to explain reinforcement. Polymer, **218**, 123513 (2021). https://doi.org/10.1016/j.polymer.2021.123513

[20] Boonstra B. B.: Mixing of carbon black and polymer: Interaction and reinforcement. Journal of Applied Polymer Science, **11**, 389–406 (1967). https://doi.org/10.1002/app.1967.070110307

[21] Medalia A. I., Laube S.: Influence of carbon black surface properties and morphology on hysteresis of rubber vulcanizates. Rubber Chemistry and Technology, **51**, 89–109 (1978). https://doi.org/10.5254/1.3535730

[22] Wootthikanokkhan J., Rattanathamwat N.: Distribution of carbon black in natural rubber/acrylic rubber blends. Journal of Applied Polymer Science, **102**, 248–256 (2006). https://doi.org/10.1002/app.23642

[23] Kaliyathan A. V., Rane A. V., Huskic M., Kunaver M., Kalarikkal N., Rouxel D., Sabu T.: Carbon black distribution in natural rubber/butadiene rubber blend composites: Distribution driven by morphology. Composites Science and Technology, **200**, 108484 (2020). https://doi.org/10.1016/j.compscitech.2020.108484

[24] Hess W. M., Scott C. E., Callan J. E.: Carbon black distribution in elastomer blends. Rubber Chemistry and Technology, **40**, 371–384 (1967). https://doi.org/10.5254/1.3539053

[25] Schwartz G. A., Cerveny S., Marzocca A. J., Gerspacher M., Nikiel L.: Thermal aging of carbon black filled rubber compounds. I. Experimental evidence for bridging flocculation. Polymer, **44**, 7229–7240 (2003). https://doi.org/10.1016/j.polymer.2003.09.007

[26] Le H. H., Hoang X. T., Schorene E., Reuter U., Stöckelhuber K. W., Mandal S., Dhakal K. N., Adhikari R., Wiessner S.: Effect of phase selective wetting of hybrid filler on the self-healing properties of rubber blends. Polymer, **231**, 124146 (2021). https://doi.org/10.1016/j.polymer.2021.124146

[27] Cataldo F.: The role of fullerene-like structures in carbon black and their interaction with dienic rubber. Fullerene Science and Technology, **8**, 105–112 (2000). https://doi.org/10.1080/10641220009351401

[28] Tarachiwin L., Sakdapipanich J., Ute K., Kitayama T., Tanaka Y.: Structural characterization of α-terminal group of natural rubber. 2. Decomposition of branch-points by phospholipase and chemical treatments. Biomacromolecules, **6**, 1858–1863 (2005). https://doi.org/10.1021/bm058004p

[29] Kawahara S., Kakubo T., Nishiyama N., Tanaka Y., Isono Y., Sakdapipanich J. T.: Crystallization behavior and strength of natural rubber: Skim rubber, deproteinized natural rubber, and pale crepe. Journal of Applied Polymer Science, **78**, 1510–1516 (2000). https://doi.org/10.1002/1097-4628(20001121)78:8<1510::AID-APP70>3.0.CO;2-4

[30] Wang P-Y., Wang Y-Z., Zhang B-L., Huang H-H.: Effect of non-rubber substances on vulcanization kinetics of natural rubber. Journal of Applied Polymer Science, **126**, 1183–1187 (2012). https://doi.org/10.1002/app.36851

[31] Smitthipong W., Tantaherdtam R., Rungsanthien K., Suwanruji P., Klanarong S., Radabutra S., Thanawan S., Vallat M. F., Nardin M., Mougin K., Chollakup M. K.: Effect of non-rubber components on properties of sulphur crosslinked natural rubbers. Advanced Materials Research, **844**, 345–348 (2003). https://doi.org/10.4028/www.scientific.net/AMR.844.345

[32] Yunyongwattanakorn J., Tanaka Y., Kawahara S., Klinklai W., Sakdapipanich J.: Effect of non-rubber components on storage hardening and gel formation of natural rubber during accelerated storage under various conditions. Rubber Chemistry and Technology, **76**, 1228–1240 (2003). https://doi.org/10.5254/1.3547799

[33] Chaikumpollert O., Yamamoto Y., Suchiva K., Kawahara S.: Protein-free natural rubber. Colloid and Polymer Science, **290**, 331–338 (2012). https://doi.org/10.1007/s00396-011-2549-y

[34] Le H. H., Abhijeet S., Ilisch S., Klehm J., Henning S., Beiner M., Sarkawi S. S., Dierkes W. K., Das A., Fischer D., Stöckelhuber K. W., Wiessner S., Khatiwadai S. P., Adhikari R., Pham T., Heinrich G., Radusch H-J.: The role of linked phospholipids in the rubber-filler interaction in carbon nanotube (CNT) filled natural rubber (NR) composites. Polymer, **55**, 4738–4747 (2014). https://doi.org/10.1016/j.polymer.2014.07.043

[35] Snowdon M. R., Mohanty A. K., Misra M.: Effect of compatibilization on biobased rubber-toughened poly (trimethylene terephthalate): Miscibility, morphology, and mechanical properties. ACS Omega, **3**, 7300–7309 (2018). https://doi.org/10.1021/acsomega.8b00490

[36] Le H. H., Hait S., Das A., Wießner S., Stöckelhuber K. W., Böhme F., Reuter U., Naskar K., Heinrich G., Radusch H-J.: Self-healing properties of carbon nanotube filled natural rubber/bromobutyl rubber blends. Express Polymer Letters, **11**, 230–242 (2017). https://doi.org/10.3144/expresspolymlett.2017.24

[37] Jönsson U., Malmqvist M., Rönnberg I.: Immobilization of immunoglobulins on silica surfaces. Stability. Biochemistry Journal, **227**, 363–371 (1985). https://doi.org/10.1042/bj2270363

[38] Le H. H., Ilisch S., Heidenreich D., Wutzler A., Radusch H-J.: Kinetics of the phase selective localization of silica in rubber blends. Polymer Composites, **31**, 1701–1711 (2010). https://doi.org/10.1002/pc.20960

[39] Le H. H., Ali Z., Uthardt M., Ilisch S., Radusch H-J.: Effect of the cross-linking process on the electrical resistivity and shape-memory behavior of cross-linked carbon black filled ethylene-octene copolymer. Journal of Applied Polymer Science, **120**, 2138–2145 (2011). https://doi.org/10.1002/app.33388

[40] Li Q., Feke D. L., Manas-Zloczower I.: Influence of aggregate structure and matrix infiltration on the dispersion behavior of carbon black agglomerates. Rubber Chemistry and Technology, **68**, 836–841 (1995). https://doi.org/10.5254/1.3538779

[41] Le H. H., Keller M., Hristov M., Ilisch S., Xuan T. H., Do Q. K., Pham T., Stöckelhuber K-W., Heinrich G., Radusch H-J.: Selective wetting and localization of silica in binary and ternary blends based on styrene butadiene rubber, butadiene rubber, and natural rubber. Macromolecular Materials and Engineering, **298**, 1085–1099 (2013). https://doi.org/10.1002/mame.201200307

[42] Puretzky A. A., Geohegan D. B., Jesse S., Ivanov I. N., Eres G.: *In situ* measurements and modeling of carbon nanotube array growth kinetics during chemical vapor deposition. Applied Physics A, **81**, 223–240 (2005). https://doi.org/10.1007/s00339-005-3256-7

[43] Wang T., Jeppson K., Liu J.: Dry densification of carbon nanotube bundles. Carbon, **48**, 3795–3801 (2010). https://doi.org/10.1016/j.carbon.2010.06.042

[44] Chapman A. V.: Natural rubber and NR-based polymers: Renewable materials with unique properties. in '24th international H.F. Mark-symposium Advances in the Field of Elastomers and Thermoplastic Elastomers. Vienna, Austria' 1–19 (2007).

[45] Luo Y. Y., Wang Y. Q., Zhong J. P., He C. Z., Li Y. Z., Peng Z.: Interaction between fumed-silica and epoxidized natural rubber. Journal of Inorganic and Organometallic Polymers and Materials, **21**, 777–783 (2011). https://doi.org/10.1007/s10904-011-9539-x

[46] Kongkaew C., Dokkhan C., Pattanawanidchai S., Chaikumpollert O., Loykulnant S.: Factors affecting creaming efficiency of bio-based polymers, vulcanization and mechanical properties of creamed skim rubber. Biomass and Bioenergy, **46**, 233–241 (2012). https://doi.org/10.1016/j.biombioe.2012.08.021

[47] Polo-Luque M. L., Simonet B. M., Valcárcel M.: Functionalization and dispersion of carbon nanotubes in ionic liquids. Trends in Analytical Chemistry, **47**, 99–110 (2013). https://doi.org/10.1016/j.trac.2013.03.007

[48] Jurkiewicz K., Pawlyta M., Burian A.: Structure of carbon materials explored by local transmission electron microscopy and global powder diffraction probes. C-Journal of Carbon Research, **4**, 68–116 (2018). https://doi.org/10.3390/c4040068

[49] Ma J. C., Dougherty D. A.: The cation-π interaction. Chemical Reviews, **97**, 1303–1324 (1997). https://doi.org/10.1021/cr9603744

[50] Fukushima T., Aida T.: Ionic liquids for soft functional materials with carbon nanotubes. Chemistry European Journal, **13**, 5048–5058 (2007). https://doi.org/10.1002/chem.200700554

[51] Narongthong J., Le H. H., Das A., Sirisinha C., Wießner S.: Ionic liquid enabled electrical-strain tuning capability of carbon black based conductive polymer composites for small-strain sensors and stretchable conductors. Composites Science and Technology, **174**, 202–211 (2019). https://doi.org/10.1016/j.compscitech.2019.03.002

[52] Brennan J. J., Jermyn T. E., Boonstra B. B.: Carbon black-polymer interaction: A measure of reinforcement. Journal Applied Polymer Science, **8**, 2687–2706 (1964). https://doi.org/10.1002/app.1964.070080615

[53] Wang M. J.: Effect of polymer-filler and filler-filler interactions on dynamic properties of filled vulcanizates. Rubber Chemistry and Technology, **71**, 520–589 (1998). https://doi.org/10.5254/1.3538492

[54] Stöckelhuber K. W., Das A., Jurk R., Heinrich G.: Contribution of physico-chemical properties of interfaces on dispersibility, adhesion and flocculation of filler particles in rubber. Polymer, 51, 1954–1963 (2010). https://doi.org/10.1016/j.polymer.2010.03.013